Spectrally resolved multidepth fluorescence imaging

Citation: Luo, Yuan et al. "Spectrally Resolved Multidepth Fluorescence Imaging." Journal of Biomedical Optics 16.9 (2011): 096015. Web. 15 Feb. 2012. © 2011 SPIE - International Society for Optical Engineering

As Published: http://dx.doi.org/10.1117/1.3626211

Publisher: SPIE - International Society for Optical Engineering

Persistent URL: http://hdl.handle.net/1721.1/69123

Version: Final published version: final published article, as it appeared in a journal, conference proceedings, or other formally published context

Journal of Biomedical Optics

SPIEDigitalLibrary.org/jbo

Spectrally resolved multidepth fluorescence imaging

Yuan Luo
Ioannis K. Zervantonakis
Se Baek Oh
Roger D. Kamm
George Barbastathis

SPIE

Spectrally resolved multidepth fluorescence imaging

Yuan Luo,[a,b] Ioannis K. Zervantonakis,[a] Se Baek Oh,[a] Roger D. Kamm,[a,c,d] and George Barbastathis[a,d]
[a]Massachusetts Institute of Technology, Department of Mechanical Engineering, Cambridge, Massachusetts 02139
[b]National Taiwan University, College of Medicine, Center for Optoelectronic Biomedicine, 10051, Taiwan
[c]Massachusetts Institute of Technology, Department of Biological Engineering, Cambridge, Massachusetts 02139
[d]Singapore-MIT Alliance for Research and Technology (SMART) Centre, 117543 Singapore

Abstract. We present a multicolor fluorescence imaging modality to visualize in real-time tissue structures emitting multispectral fluorescent light from different focal depths. Each designated spectrum of fluorescent emission from a specific depth within a volumetric tissue is probed by a depth-spectrum selective holographic grating. The grating for each fluorescent color are multiplexed within a volume hologram, which enables simultaneously obtaining multicolored fluorescent information at different depths within a biological tissue sample. We demonstrate the imaging modality's ability to obtain laser-induced multicolored fluorescence images of a biological sample from different depths without scanning. We also experimentally demonstrate that the imaging modality can be simultaneously operated at both fluorescent and bright field modes to provide complementary information of volumetric tissue structures at different depths in real-time.
[DOI: 10.1117/1.3626211]

Keywords: holography; diffractive optics; holographic optical elements; multiplexed hologram; volume hologram; three-dimensional image acquisition; fluorescence.

Paper 11134R received Mar. 20, 2011; revised manuscript received Jul. 15, 2011; accepted for publication Jul. 27, 2011; published online Sep. 9, 2011.

1 Introduction

Laser-induced fluorescence has been developed as a primary imaging technique in many areas of biology, material science, and medical applications because of its sensitivity, targeting selectivity, and specificity. The emission characteristics of many fluorescent makers and probes used for imaging are affected by the volumetric environment within an object. Therefore, much effort has been involved in developing and improving fluorescence three-dimensional (3D) imaging systems providing the ability to determine properties of the volumetric environment in a spatially and spectrally resolved manner.

Some conventional 3D imaging systems such as scanning confocal microscopy[1,2] and optical coherence tomography (OCT)[3–5] would ideally provide 3D images, enabling characterization of a volume of tissue. However, all these systems have complex mechanical designs, requiring scanning in two lateral dimensions and depth focusing. In addition, although some OCT systems have fast scan rates, OCT is a coherent imaging technique and cannot provide fluorescence information.

Recently, a variety of holographic techniques has been successfully applied to 3D fluorescence imaging applications. These techniques include scanning fluorescence holography[6–8] and wide-field holographic microscopy.[9–13] The most recent examples of wide-field holographic microscopy for 3D fluorescence imaging are FINCH digital holography[10,11] proposed by Rosen and volume holography proposed by our group.[13] In the former, FINCH fluorescence color holography can simultaneously obtain different fluorescent colors from multiple depths but it requires intensive computation and complicated data analysis. The latter technique is limited to obtaining only a single fluorescent color from multiple depths within an object.

In this paper, we present a depth-spectrum selective volume holographic imaging (DS-VHI) system based on the wavelength coded technique[14] for color fluorescence imaging. The DS-VHI system incorporates a depth-spectrum selective multiplexed volume hologram (MVH) to simultaneously obtain different fluorescent colors from multiple planes in real-time. Each multiplexed grating within the hologram is sensitive to a specific depth. Each depth within a tissue sample is probed by its corresponding fluorescent color and projected to a distinct lateral location on a digital camera. This is particularly beneficial for 3D fluorescence imaging to take advantage of its deeper penetration, and it gives DS-VHI improved contrast and penetration depth.

The DS-VHI system has significant advantages over previous fluorescence imaging systems in that it does not require intensive computational reconstruction technique, and can obtain multiple depth-resolved and fluorescent information of an object in real-time. In contrast to the fluorescent imaging system in Ref. 15 using diffractive optical elements based on chromatic aberration techniques, DS-VHI provides more freedom to probe an arbitrary arrangement of fluorescent colors in different depths using appropriately depth-spectrum selective holograms. DS-VHI offers higher efficiency with minimal crosstalk as more gratings are multiplexed into the hologram. In addition, the DS-VHI can provide both fluorescent and bright field information of tissue structures from different depths in real-time without scanning.

In Sec. 2, we introduce the basic principles of the DS-VHI system by utilizing the Bragg degeneracy property. In Sec. 3, laser-induced multicolored fluorescence images of human breast cancer cells within a 3D biological matrix at different depths are

Address all correspondence to: Se Baek Oh, Massachusetts Institute of Technology, Mechanical Engineering, Room 3-473m, 77 Massachusetts Avenue, Cambridge, Massachusetts 02139; Tel: 240-688-2474; E-mail: sboh@alum.mit.edu.

1083-3668/2011/16(9)/096015/5/$25.00 © 2011 SPIE

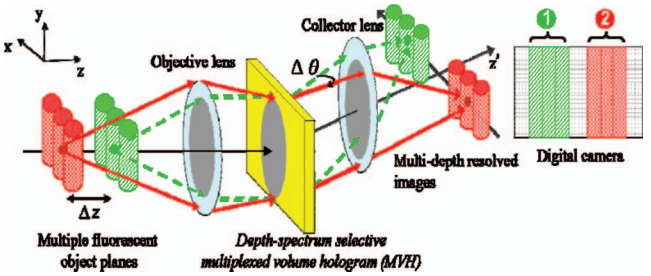

Fig. 1 Schematic setup of the DS-VHI system. Multicolor fluorescent planes within a tissue sample are simultaneously obtained by a depth-spectrum selective MVH and laterally displayed on a digital camera.

obtained by the DS-VHI system in real-time without scanning. We also experimentally demonstrate the DS-VHI system can be operated at both fluorescent and nonfluorescent modes to provide complementary information of tissue structures at different depths in real-time. In Sec. 4, we present our findings of the DS-VHI system.

2 Principles of DS-VHI

Figure 1 shows the operation of the DS-VHI system that is imaging a multispectral fluorescent object illuminated using laser excitation. Different spectrum illustrates the longer and shorter fluorescent wavelengths of the object's emission light from different depths within a biological sample. The system consists of a 4-*f* configuration of lenses with a depth-spectrum selective MVH in the central (Fourier) plane. Each multiplexed grating within the depth-spectrum selective MVH selects a specific depth by its corresponding wavelength and displays on a digital camera at a different lateral location. In our approach, a longer wavelength is designated into a deeper depth, allowing greater imaging penetration within a biological tissue sample.

To understand the operational principle, we utilize *k*-sphere formulation[16] to analyze the system. Figures 2(a) and 2(b) show the resultant *k*-sphere diagrams for two multiplexed gratings within MVH in the DS-VHI system in 3D and two-dimensional space. Two incident beams with respective red and green color propagate along the optical axis (z) and diffract to a different angle after being Bragg matched to its corresponding multiplexed grating within the MVH. Therefore, each depth-spectrum selective grating creates an image from wavefronts that originate at a particular depth with a specific color emitting from the object while rejecting all other wavefronts. This significantly improves image contrast with minimal crosstalk when attempting to image a volumetric object. The propagation vectors of incident and diffracted beams at the Bragg condition can be expressed as:

$$k_{\mathrm{diff},i} - k_{\mathrm{prob},i} = K_i, \quad \text{and} \quad i = 1, 2 \ldots, N. \tag{1}$$

$|k_{\mathrm{diff},i}| = |k_{\mathrm{prob\_}i}| = 2\pi n/\lambda_{\mathrm{prob},i}$. n is the refractive index of the recording material, and λ is wavelength in free space. N is the number of multiplexed gratings. In this case, $N = 2$, and K_1 and K_2 are the grating vectors for probe in green and red wavelength, respectively.

Due to Bragg degeneracy property,[17] a volume holographic grating probed at one wavelength can be formed at another wavelength. Figure 3(a) illustrates the first multiplexed grating probed by green color light ($\lambda_{\mathrm{prob},1} = 520$ nm) and recorded

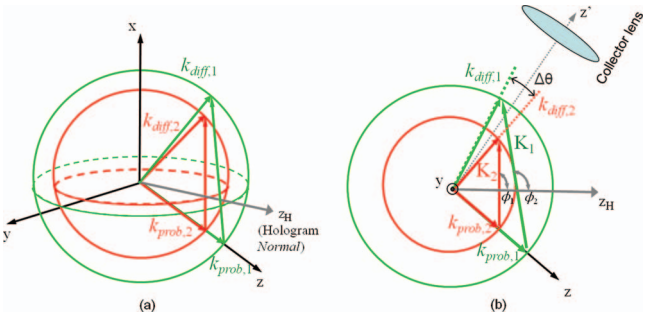

Fig. 2 (a) Geometric construction of a 3D *k*-sphere diagram of two multiplexed gratings within a depth-spectrum selective MVH in the DS-VHI. (b) The geometry of the resultant *k*-sphere representation and collector lens on the *x*-*z* plane (side view from the *y*-axis). Red and green fluorescent beams emitted from different object planes along a common axis are probed by their corresponding gratings at the spectrum of 620 and 520 nm.

using in degenerate fashion by a blue color laser ($\lambda_{\mathrm{rec},1} = 488$ nm). Figure 3(b) illustrates the second grating probed by red color light ($\lambda_{\mathrm{prob},2} = 620$ nm) and recorded using in degenerate fashion by the same blue color laser ($\lambda_{\mathrm{rec},2} = 488$ nm). The relationship between interbeam angles in Figs. 3(a) and 3(b) can be given as

$$\theta_{\mathrm{prob},i} = \phi_i - \cos^{-1}\left[\frac{\lambda_{\mathrm{prob},i}}{\lambda_{\mathrm{rec},i}}\cos(\phi_i - \theta_{\mathrm{sig},i})\right]. \tag{2}$$

Figure 3(c) shows multiplexing these two gratings within a hologram forming a depth-spectrum selective MVH using one recording laser in blue color. Without adjusting the reference beam during exposure in recording, an angle of signal beam is changed by $\Delta\theta_{\mathrm{rec};i,i+1}$. An additional hologram rotation angle ($\Delta\psi_{i,i+1}$) is also necessary because this is done to maintain the same incident beam angle while using different wavelengths for probe. The rotation angles of hologram and signal beam between exposures can be expressed as:

$$\Delta\theta_{\mathrm{rec};i,i+1} = \theta_{\mathrm{rec},i+1} - \theta_{\mathrm{rec},i}, \tag{3}$$

and

$$\Delta\psi_{i,i+1} = \Delta\theta_{\mathrm{rec};i+1,i}/2 + (\phi_i - \phi_{i+1}), \tag{4}$$

where ψ_i and ψ_{i+1} are the angles of the i'th and $i+1$'th multiplexed grating vectors with respect to its corresponding hologram normal.

3 Experimental Results

3.1 *Fabrication of Depth-Spectrum Selective MVH*

In our approach, phenanthrenquinone (PQ)- doped polymethylmethacrylate (PMMA) polymer material is used as the recording material since it can be fabricated in a variety of forms and thickness.[18] With proper fabrication process,[18] the holograms were formed in 1.8-mm thick samples, and can provide very fine wavelength selectivity with less than 1 nm spectral resolution. However, PQ-PMMA is particularly sensitive in a 450 to 500 nm band.[19] Both gratings are recorded using an Argon ion laser operating at a single wavelength (488 nm) as shown in Fig. 4, providing a simple setup based on Bragg degeneracy instead of using multiple or tunable lasers. A laser beam is split

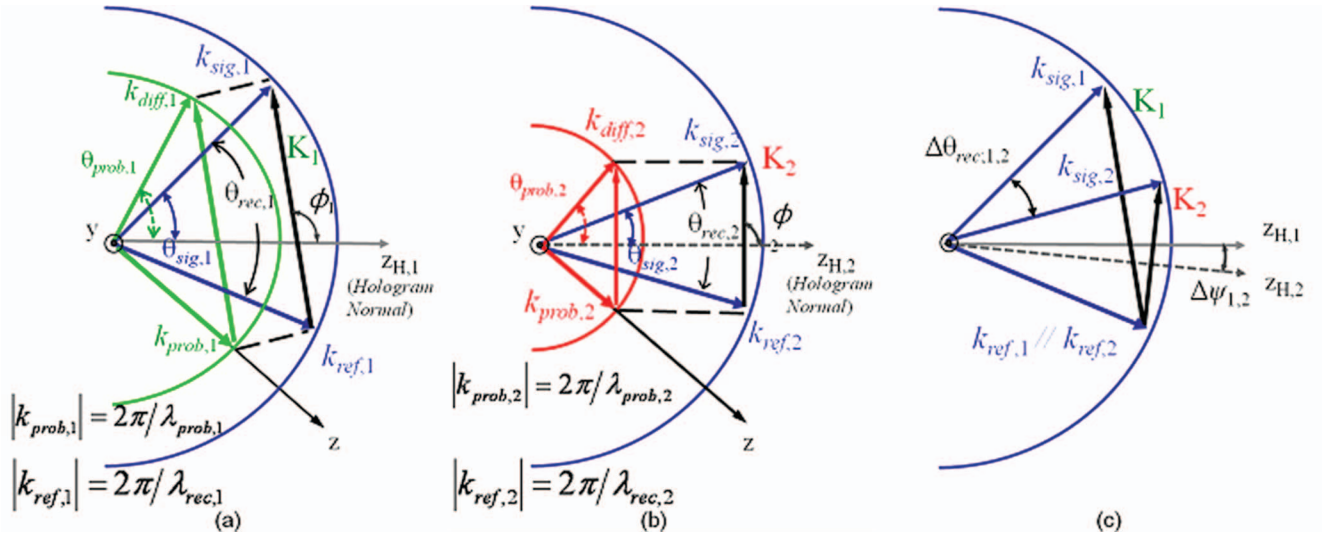

Fig. 3 (a) A *k*-sphere diagram for grating recording geometry with a blue laser ($\lambda_{rec,1}$ = 488 nm) and probing with green wavelength ($\lambda_{prob,1}$ = 520 nm). (b) A *k*-sphere diagram for grating recording geometry with a blue laser ($\lambda_{rec,2}$ = 488 nm) and probing with green wavelength ($\lambda_{prob,2}$ = 620 nm) (c) The analysis of multiplexing these gratings using one blue laser with the same reference beam angle in recording.

into a reference and signal arm. A collimated beam is formed in the signal arm while a point source is formed in the reference arm, and its position is adjusted by Δz relative to the recording material for each exposure. In addition, the angle of the signal beam and angle of the hologram are changed by $\Delta\theta_{\text{rec};i,i+1}$ and $\Delta\psi_{i,i+1}$, as we noted earlier.

In our experiment, the NA of the objective as shown in Fig. 4 is 0.55. The axial displacement is $\Delta z = 30\ \mu$m. The nominal angles in air are $\psi_1 = 91$ deg and $\psi_2 = 89.5$ deg. The angles of the interbeam and hologram for the first grating in recording are $\theta_{\text{rec},1} = 60.5$ deg and $\psi_1 = 29.2$ deg. The corresponding signal beam angle for recording in 488 nm and probing in 520 nm is $\theta_{\text{sig},1} = 31.3$ deg and $\theta_{\text{prob},1} = 33.5$ deg, respectively. The rotation angles of the signal beam and hologram for the second multiplexed grating in recording are $\Delta\theta_{\text{rec};1,2} = -12.7$ deg and $\Delta\psi_{1,2} = 4.85$ deg, and the corresponding signal beam angle for probing in 620 nm is $\theta_{\text{prob},2} = 30.5$ deg.

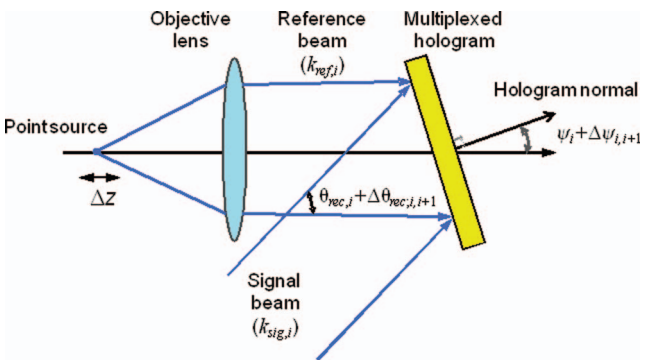

Fig. 4 Experimental recording setup to multiplex depth-spectrum selective gratings within a volume hologram. An argon ion laser beam is split into a reference and signal arm for each exposure. $k_{\text{sig},i}$, and $k_{\text{ref},i}$ are the wave vectors of the recording signal and reference beams for the first grating when $i = 1$ and the second grating when $i = 2$.

3.2 *Image Acquisition*

An experimental setup of the DS-VHI system was carried out in Fig. 1. An Olympus ULWDMSPlan50X was used for the objective lens and a Mitutuyo MPlanAPO20X for the collector lens in the system with a QImaging CCD camera (QIC-F-CLR-12C). A depth-spectrum selective MVH consisted of two multiplexed gratings with diffraction efficiencies of approximately 30% at 488 nm. The angle separation ($\Delta\theta$) between two diffracted beams was 3 deg.

To evaluate the spatial resolution of the DS-VHI system, a phantom sample was prepared with spatial features formed in glass that were filled with a fluorescent quantum dot solution (Evident Technologies ED-C11-TOL-0620). The smallest lines and the diameter of the circular patterns on the phantom are 7.5 μm, and the next larger sets of lines are 15 μm, then 30 and 60 μm lines. The circular and rectangular patterns are etched into a glass cover slip to a depth of 1 μm. The etched trenches are then filled with the quantum dot solution and capped with another cover slip. For imaging, the sample was illuminated with a 355 nm laser. The quantum dots emit light with a center wavelength around 620 nm and a spectral bandwidth of ~30 nm. The axial (depth) resolution of the DS-VHI system is approximately 15 μm with a point source generated using a collimated HeNe laser and a microscope objective placed on a motorized translation stage. Figure 5(a) shows both experimental measurements and simulation results based on rigorous coupled wave theory with ray-tracing techniques based on Ref. 20. Figure 5(b) shows the fluorescence image obtained using one of the two multiplexed gratings in the DS-VHI system. As illustrated, the fluorescence image with spatial features of at least 7.5 μm is well defined.

Figure 6(a) shows two depth-resolved fluorescence images from a 3D volumetric tissue sample with human breast cancer cells within a 3D biological matrix[21,22] using the DS-VHI system. The cancer cells were stained with two diluted fluorescent green and red quantum-dot solutions (Evident Technologies ED-C11-TOL-0520 and ED-C11-TOL-0620). The

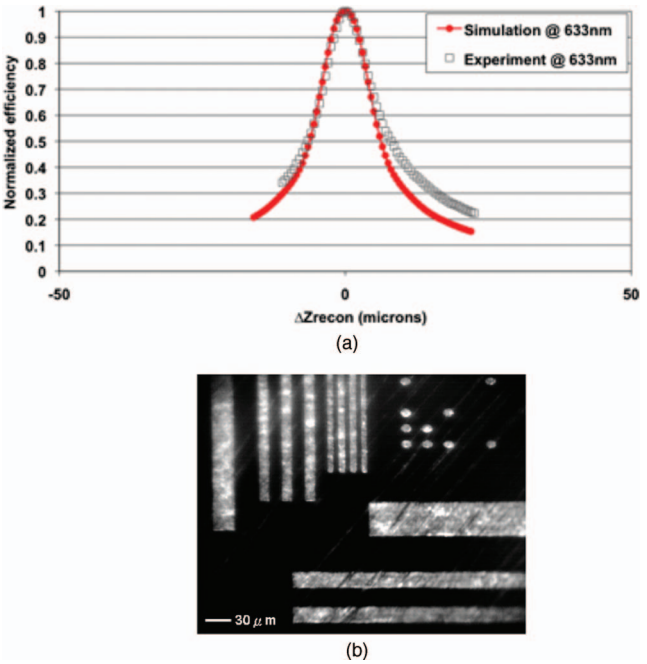

Fig. 5 (a) Experimental and numerical results of the axial selectivity at 633 nm of a DS-VHI. (b) Image of a phantom sample containing red fluorescent quantum dots arranged in circular and rectangular patterns. The image obtained with the DS-VHI system to measure the spatial resolution.

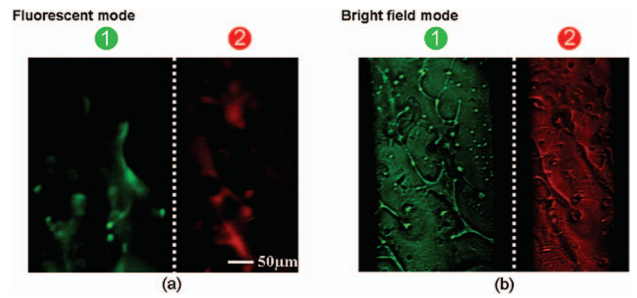

Fig. 6 Experimental results obtained from a volumetric sample with human breast cancer cells seeded in a 3D collagen type I biological matrix. (a) Fluorescence images of the sample labeled with diluted green and red fluorescent quantum dots solutions (Evident Technologies ED-C11-TOL-0520 and ED-C11-TOL-0620). The fluorescently labeled cell structures were uniformly illuminated by a 355 nm pump laser beam. (b) Two planes of the volumetric tissue sample obtained with the DS-VHI system using both green and red LEDs for illumination.

stained tissue sample was excited using a 355 nm UV pump laser and simultaneously emitted in green and red color, with respective central wavelengths of ~520 and ~620 nm and same spectral bandwidth of 40 nm. Figure 6(b) shows bright field images of the tissue sample obtained by the DS-VHI operated in bright field mode using both green and red light-emitting diodes (LEDs) for illumination. The central wavelength of the green LED is ~520 nm with a spectral bandwidth of 40 nm, and the central wavelength of the red LED is ~620 nm with a spectral bandwidth of 30 nm.

Furthermore, the DS-VHI simultaneously provides complementary information of both fluorescent and nonfluorescent tissue structures at different depths in real-time, which should offer many promising applications in basic biological and biomedical research areas. Figure 7(a) on the left shows the complementary information using a green LED and a 355 nm pump laser beam, while the figure on the right shows the image illuminated by a red LED. Figure 7(b) on the left shows the image illuminated by a green LED, while the figure on the right shows the results illuminated using a red LED and a 355 nm pump laser beam. In Fig. 7(c), two planes of the volumetric tissue sample obtained with the DS-VHI system using both bright field and fluorescent information. The images displayed on the digital camera were in gray scale; however, a MATLAB program was applied to add pseudocolor with linear gray color mapping scheme for easy visualization.

4 Conclusions

We describe a DS-VHI system for color fluorescence imaging. Our findings indicate that the depth-spectrum selectivity incorporating into an MVH in the DS-VHI can detect in real-time multiple fluorescent colors from different depths within a biological sample. In our approach, the depth separation (Δz) was ~50 μm. Phantom studies showed that 7.5 μm features were well-resolved using the DS-VHI with a phantom sample fulfilled with red quantum dots solution. In terms of depth resolution, confocal scanning systems with ~1 μm axial resolution have a much better performance than the DS-VHI. However, DS-VHI provides both spectral and axial images simultaneously without scanning. Due to high spectral resolution (less than 1 nm, as noted earlier), the DS-VHI systems can obtain different wavelengths from multiple depths, and the crosstalk will be minimal. In addition, the depth separation can be tuned by adjusting Δz in the hologram recording process, and the resolution can be

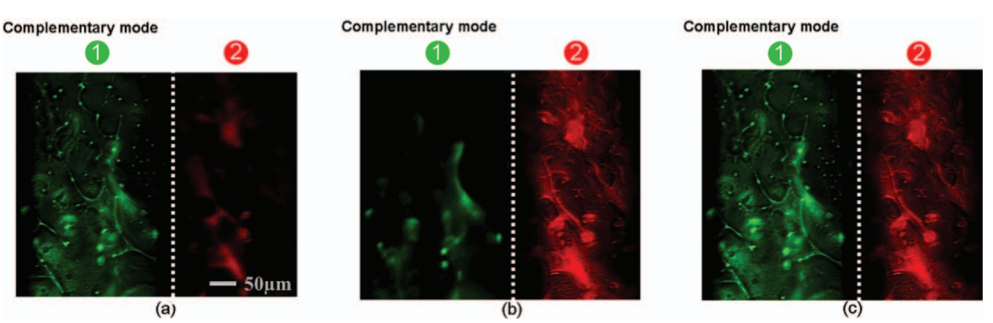

Fig. 7 Two depth-resolved images of the tissue structures obtained with the DS-MVHI system, simultaneously operated at both fluorescent and nonfluorescent modes. Complementary information of the tissue structures can be visualized in real-time.

enhanced by using higher system magnification value and increasing the volume selectivity.[23]

Due to Bragg degeneracy and hologram material properties, the depth-spectrum selective MVH can be recorded at a single wavelength instead of using a tunable laser with multiple wavelengths. PQ-PMMA recording material has been demonstrated to have up to 50 multiplexed holograms with index modulations of 3×10^{-4} (Refs. 24 and 25). With more multiplexed gratings, the DS-VHI can be also extended to use other materials[26,27] to provide more depth information, allowing us to gather more multiple depth-resolved color fluorescence images. The configuration using spatial light modulations may be programmable to provide multifocal lenses.[28] However, it cannot acquire spectral information from different depths in real-time.

Applications of our DS-VHI approach include monitoring the dynamics of cancer cell rolling and migration in real-time within a 3D microfluidic cell culture device. Moreover, the DS-VHI system has been demonstrated to simultaneously obtain complementary fluorescent and bright field images at different depths in real-time. The combined fluorescent and bright field images, including structural and spectral information, should be significantly beneficial to biomedical applications such as more specific diagnosis of disease[29] and quantitative phase imaging.[30] With a thicker hologram, the system can provide finer selectivity.[16,20] The system can also be adapted to other illumination configurations for greater axial selectivity and endoscopic format for biomedical applications.

Acknowledgments

The authors would like to thank Raymond Kostuk, Jose Castro, Erich de Leon, and John Brownlee for discussions and assistance for use of facilities to record holograms. The authors gratefully acknowledge the support from the following sponsors: the National Institutes of Health (NIH-RO1CA134424) and the Singapore-MIT Alliance for Research and Technology Centre (SMART 015824-039).

References

1. B. R. Masters, "Selected papers on confocal microscopy," SPIE Milestone Series, Volume MS 131 (1996).
2. J. B. Pawley, *Handbook of Biological Confocal Microscopy*, Springer, New York (2006).
3. D. Huang, E. A. Swanson, C. P. Lin, J. S. Schuman, W. G. Stinson, W. Chang, M. R. Hee, T. Flotte, K. Gregory, C. A. Puliafito, and J. G. Fujimoto, "Optical coherence tomography," *Science* **254**, 1178–1181 (1991).
4. J. M. Schmitt, "Optical coherence tomography (OCT): a review," *IEEE J. Sel. Top. Quantum Electron.* **5**, 1205–1215 (1999).
5. A. M. Zysk, F. T. Nguyen, A. L. Oldenburg, D. L. Marks, and S. A. Boppart, "Optical coherence tomography: a review of clinical development from bench to bedside," *J. Biomed. Opt.* **12**, 051403 (2007).
6. B. W. Schilling, T. C. Poon, G. Indebetouw, B. Storrie, K. Shinoda, Y. Suzuki, and M. H. Wu, "Three dimensional holographic fluorescence microscopy," *Opt. Lett.* **22**, 1506–1508 (1997).
7. G. Indebetouw and W. W. Zhong, "Scanning holographic microscopy of three-dimensional fluorescent specimens," *J. Opt. Soc. of Am. A* **23**, 1699–1707 (2006).
8. J. Rosen, G. Indebetouw, and G. Brooker, "Homodyne scanning holography," *Opt. Express* **14**, 4280–4285 (2006).
9. W. Xu, M. H. Jericho, H. J. Kreuzer, and I. A. Meinertzhagen, "Tracking particles in four dimensions with inline holographic microscopy," *Opt. Lett.* **28**, 164–166 (2003).
10. J. Rosen and G. Brooker, "Fluorescence incoherent color holography," *Opt. Express* **15**, 2244–2250 (2007).
11. J. Rosen and G. Brooker, "Non-scanning motionless fluorescence three-dimensional holographic microscopy," *Nat. Photonics* **2**, 190–195 (2008).
12. W. Liu, D. Psaltis, and G. Barbastathis, "Real-time spectral imaging in three spatial dimension," *Opt. Lett.* **27**, 854–856 (2002).
13. Y. Luo, P. J. Gelsinger-Austin, J. M. Watson, G. Barbastathis, J. K. Barton, and R. K. Kostuk, "Laser induced fluorescence imaging of sub-surface tissue structures with a volume holographic spatial-spectral imaging system," *Opt. Lett.* **33**, 2098–2100 (2008).
14. Y. Luo, S. Oh, and G. Barbastathis, "Wavelength-coded multi-focal microscopy," *Opt. Lett.* **35**, 781–783 (2010).
15. P. A. Dalgarno, H. I. C. Dalgarno, A. Putoud, R. Lambert, L. Paterson, D. C. Logan, D. P. Towers, R. J. Warburton, and A. H. Greenaway, "Multiplane imaging and three dimensional nanoscale particle tracking in biological microscopy," *Opt. Express* **18**, 877–884 (2010).
16. G. Barbastathis and D. Psaltis, "Volume holographic multiplexing methods," in *Holographic Data Storage*, Springer, Berlin (2000).
17. J. Goodman, *Introduction to Fourier Optics*, 3rd Ed., pp. 336–346, Roberts and Company, Englewood (2005).
18. Y. Luo, P. J. Gelsinger, G. Barbastathis, J. K. Barton, and R. K. Kostuk, "Optimization of multiplexed holographic gratings in PQ-PMMA for spectral-spatial filters," *Opt. Lett.* **33**, 566–568 (2008).
19. J. M. Russo, "Temperature dependence of holographic filers in phenanthrenquinone-doped poly(methyl methacrylate)," ECE Department, Thesis, The University of Arizona (2007).
20. Y. Luo, J. M. Castro, J. K. Barton, R. K. Kostuk, and G. Barbastathis, "Simulations and experiment of aperiodic and multiplexed gratings in volume holographic imaging systems," *Opt. Express* **19**, 19273–19285 (2010).
21. S. Chung, R. Sudo, P. J. Mack, C. Wan, V. Vickerman, and R. Kamm, "Cell migration into scaffolds under co-culture conditions in a microfluidic platform," *Lab Chip* **9**, 269–275 (2009).
22. S. Chung, R. Sudo, V. Vickerman, I. K. Zervantonakis, and R. D. Kamm, "Microfluidic platforms for studies of angiogenesis, cell migration, and cell-cell interactions," *Sixth International Bio-Fluid Mechanics Symposium and Workshop*, Pasadena, California (2008); *Ann. Biomed. Eng.* **38**, 1164–1177 (2010).
23. Y. Luo, J. M. Russo, R. K. Kostuk, and G. Barbastathis, "Silicon oxide nanoparticles doped PQ-PMMA for volume holographic imaging filters," *Opt. Lett.* **35**, 1269–1271 (2010).
24. G. J. Steckman, I. Solomatine, G. Zhou, and D. Psaltis, "Holographic data storage in phenanthrenequinone doped PMMA," *Proc. SPIE* **3623**, 234–242 (1999).
25. S. H. Lin, K. Y. Hsu, W-Z Chen, and W. T. Whang, "Phenanthrenequinone-doped poly(methyl methacrylate) photopolymer bulk for volume holographic data storage," *Opt. Lett.* **25**(7), 451–453 (2000).
26. N. Suzuki, Y. Tomita, K. Ohmori, M. Hidaka, and K. Chikama, "Highly transparent ZrO_2 nanoparticle-dispersed acrylate photopolymers for volume holographic recording," *Opt. Express* **14**, 12712–12719 (2006).
27. S. Tay, P. A. Blanche, R. Voorakaranam, A. V. Tunc, W. Lin, S. Rokutanda, T. Gu, D. Flores, P. Wang, G. Li, P. St Hilaire, J. Thmoas, R. A. Norwood, M. Yamamoto, and N. Peyghambarian, "An updatable holographic three-dimensional display," *Nature* **451**, 694–698 (2008).
28. C. Maurer, S. Khan, S. Fassl, S. Bernet, and M. Ritsch-Marte, "Depth of field multiplexing in microscopy," *Opt. Express* **18**, 3023–3034 (2010).
29. R. V. Kuranov, V. V. Sapozhnikova, H. M. Shakhova, V. M. Gelikonov, E. V. Zagainova, and S. A. Petrova, "Combined application of optical methods to increase the information content of optical coherent tomography in diagnostics of neoplastic processes," *Quantum Electron.* **32**, 993–998 (2002).
30. L. Waller, Y. Luo, S. Y. Yang, and G. Barbastathis, "Transport of intensity phase imaging in a volume holographic microscope," *Opt. Lett.* **35**, 2961–2963 (2010).